Persistence and phase synchronisation properties of fixational eye movements

S. Moshel[1,a], A.Z. Zivotofsky[2], L. Jin-Rong[3], R. Engbert[4], J. Kurths[5], R. Kliegl[4], and S. Havlin[1]

[1] Minerva Center & Department of Physics, Bar-Ilan University, Ramat Gan 52900, Israel
[2] Gonda Brain Research Center, Bar-Ilan University, Ramat-Gan 52900, Israel
[3] Department of Mathematics, East China Normal University, Shanghai 200062, PR China
[4] Department of Psychology, University of Potsdam, PO Box 601553, 14415 Potsdam, Germany
[5] Department of Physics, University of Potsdam, PO Box 601553, 14415 Potsdam, Germany

Abstract. When we fixate our gaze on a stable object, our eyes move continuously with extremely small involuntary and autonomic movements, that even we are unaware of during their occurrence. One of the roles of these fixational eye movements is to prevent the adaptation of the visual system to continuous illumination and inhibit fading of the image. These random, small movements are restricted at long time scales so as to keep the target at the centre of the field of view. In addition, the synchronisation properties between both eyes are related to binocular coordination in order to provide stereopsis. We investigated the roles of different time scale behaviours, especially how they are expressed in the different spatial directions (vertical versus horizontal). We also tested the synchronisation between both eyes. Results show different scaling behaviour between horizontal and vertical movements. When the small ballistic movements, i.e., microsaccades, are removed, the scaling behaviour in both axes becomes similar. Our findings suggest that microsaccades enhance the persistence at short time scales mostly in the horizontal component and much less in the vertical component. We also applied the phase synchronisation decay method to study the synchronisation between six combinations of binocular fixational eye movement components. We found that the vertical-vertical components of right and left eyes are significantly more synchronised than the horizontal-horizontal components. These differences may be due to the need for continuously moving the eyes in the horizontal plane in order to match the stereoscopic image for different viewing distances.

1 Introduction

1.1 Eye movements during fixation

The human visual system seems to have a built-in paradox: In order to inspect the minute details of the world it must stabilise gaze; yet if it were to fixate for an extended period, the entire visual world would fade from view due to neural adaptation. Images that are experimentally stabilised on the retina of awake humans fade quickly and are no longer seen [1]. This is in line with the general principle that the nervous system responds to change and eschews constant stimulation, to which it readily adapts.

Miniature eye movements (discussed below) are generally assumed to prevent the adaptation of the visual system by their small random displacements [2]. Early experiments dating back

---

[a] e-mail: `moshels@shoshi.ph.biu.ac.il`

over 50 years discovered this phenomenon and detected fading on the time scale of several seconds. More recent studies have found that even much shorter periods of visual stabilisation lead to a significant decrease in visibility [3]. Coppola and Purves [4] found that some images can disappear in less than 80 ms.

Fixational eye movements cause the image of an object to constantly stimulate new cells in the fovea [5]. Three classes of eye movements occur during visual fixation. These movements are: (i) high-frequency, small-amplitude tremor, (ii) slow drift, and (iii) fast microsaccades [3,6] (see Figs. 1 and 6(b)). These movements are generally assumed to counteract the adaptation of the visual system by their small random displacements, although their role in the visual process is not yet fully understood [2,7].

Tremor (or physiological *nystagmus*[1]) are high-frequency (up to 90 Hz) oscillation of the eye, typically with an amplitude less than 0.01 deg. Tremor causes the image of an object to constantly stimulate new cells in the retina [3]. Tremor is generally thought to be independent in the two eyes. This imposes a physical limit on the ability of the visual system to match corresponding points in the retina [8,9].

Drifts are slow movement episodes, with a mean amplitude of 0.04 to 0.13 deg on average [3], away from a fixation point. Tremor is superimposed on drift and occurs during the epochs between microsaccades (for microsaccades see next paragraph). Initially, drifts were assumed to be random motions of the eye [10], generated by the instability of the ocular motor system [3,11]. However, recently it was found that drifts have a compensatory role in maintaining accurate visual fixation in the absence of microsaccades, or at times when compensation by microsaccades is relatively poor [11–15]. If drifts and tremor are indeed conjugate, this might indicate that they have a central origin (at least in part). This idea is supported by observations of reduced or absent tremor in patients with brain-stem lesions [16].

Microsaccades are rapid small amplitude movements ranging between 0.02 and 1 deg, with a duration of about 25 ms, and occur at a typical mean rate of 1 to 2 per second [17]. They seem to reposition the eye on the target, however, a simple error-correcting function could not be demonstrated [2]. Microsaccades have been described in several species other than humans [18]. However, they seem to be most important in species with foveal vision (such as monkeys and humans). One of the possible roles of microsaccades is to correct displacements in eye position produced by drifts [10,11]. Recently, it was found that microsaccades are triggered dynamically by low retinal image slip [19]. Microsaccades might help to counteract receptor adaptation on a short timescale and to correct fixation errors on a longer timescale [2,20].

Drift and tremor movements are rather irregular and show statistical properties of a correlated random walk [20,21] (for a first model of fixational eye movements see Ref. [22]). Microsaccades, however, create more linear movement segments embedded in the eyes' trajectories during fixational movements. There is evidence that microsaccades are persistent and anti-persistent at different time scales [2,20]. They enhance the persistence at short time scales mostly in the horizontal component and much less in the vertical component. This difference may be due to the need to continuously move the eyes in the horizontal plane in order to match the stereoscopic image for different viewing distances [20]. Microsaccades show a characteristic signature of rate suppression and rate enhancement in response to visual change [17,23], and are modulated by covert shifts of attention [17].

In the current work we demonstrate the persistence and synchronisation properties of the different fixational eye movement components (horizontal and vertical). We show that the horizontal movements have different persistence properties than the vertical ones, mainly due to the effect of the microsaccades. We also present the synchronisation properties between the eye movement components. We tested the synchronisation properties between the two eyes, and found that synchronisation exists only between the right and left horizontal components and the right and left vertical components. No synchronisation was found between horizontal and vertical. Moreover, the vertical components were significantly more synchronised than the horizontal [24].

---

[1] *Nystagmus*: Involuntary rhythmical oscillations of one or both eyes.

1.2 The dynamics of fixational eye movements

The multi-time-scale behaviour of fixational eye movements is not fully understood and in this study we investigate this behaviour.

Statistical physics enables us to pose this issue in an appropriate quantitative fashion. The equivalent approaches in physics in tracking physiological functionality may reveal the sub-components of a physiological complex system and define their dynamical dependence upon each other. In such situations there will generally be nonlinear feedback mechanisms that make the dynamics more persistent than complete randomness. Another feature, which is also observed frequently in such situations, is the partial synchronisation between parts of the complex system.

We first discuss long-term memory. The behaviour of each of the fixational eye movements might be completely random, which usually suggests a lack of functionality. On the other hand it might be that these mechanisms have some stochastic motion which depends on the past movements to a certain extent. If the dependence of the motion on its past decays slower than exponentially, physicists tend to relate such a behaviour to the existence of a control system with complex feedback mechanisms which carries information about past events. Such a quantity is intuitively preferred because the eye, on the one hand, has to counteract fading of the retinal cell response (which explains the erratic movement) and, on the other hand, enable the brain to track a target (which explains why the movement should have some persistence, unlike a conventional random walk).

Engbert et al. [2] studied the persistence properties of fixational eye movement trajectories. They tested the correlation properties of the trajectory's displacement vector $\Delta\boldsymbol{r}_i$ via calculating the mean square displacement $\langle \Delta r^2 \rangle$ applying the Hurst's exponent method. The trajectories were found to obey a scaling law $\langle \Delta r^2 \rangle \sim \Delta t^H$, where $H = 2\alpha$. They studied trajectories both with and without microsaccades. They found that the scaling exponent α for trajectories that include microsaccades shows persistence properties in short time scales (between 2–20 ms) and anti-persistence in long time scales (between 100–400 ms). However, after filtering out the microsaccades, in short time scales the trajectories remained persistent while in long time ranges they approach random behaviour. They concluded that microsaccades may play a key role in correcting fixation position and controlling binocular disparity.

On short time scales, up to 20 ms, microsaccades may help to counteract retinal adaptation [1,10] by increasing the persistence of the eye's "random walk". On long time scales, however, microsaccades behave as error reducing (relative to an uncorrelated random walk) for fixation positions of the eyes, as well as for binocular disparity. Nevertheless, the function of microsaccades remains puzzling, because microsaccades can be voluntarily suppressed [25].

To address further aspects of this subject, we studied the different roles of the horizontal and vertical movements. We hypothesised that a tendency of the movement to be more persistent in one component than in the other one is enough in order to claim that their roles are different, and even to try to identify the main functionality of each component.

Another outcome of such a separation will be the ability to partially explain Engbert's observed separation of scales. We will further follow in Engbert's footsteps on that subject and try to speculate about the role of microsaccades. In fact, we claim that the significantly different dynamics of the two spatial components are mainly due to microsaccades. This result is in good agreement with the neurophysiological fact that horizontal and vertical components of saccades are controlled by different brain stem nuclei [26].

In many pathological states the fixation system can be disrupted by slow drift, nystagmus, or involuntary saccades. However, because all three of them also occur in healthy individuals, it is difficult to determine if there is truly an abnormality present. Our results about the normal eye movements in the fixational system may be useful in clinical evaluation of such dysfunctions.

Next we discuss synchronisation patterns. Synchronisation of fixational eye movements is not trivial to identify because these movements have complex random walk-like characteristics. These movements are assumed to serve several functions [3,17]. Many animals with laterally-placed eyes, such as chameleons, move their eyes independently of one another. In contrast, in primates, such as humans, with frontally placed eyes, their binocular vision critically depends on the coordination of the two eyes so that the two foveas are pointed at the same point in visual space.

A key question is related to a controversy in the 19th century between Ewald Hering and Hermann von Helmholtz [27]: Hering argued that binocular coordination was innate, whereas Helmholtz took the position that each eye moves independently and binocular coordination is learned. Recent results regarding the neural control of eye movements supports Helmholtz's contention [28].

Fixational eye movements occur involuntarily and unconsciously during visual fixation of stationary targets [29]. Here we address the synchronisation properties of the fixational eye movements of both eyes. Because of the complex behaviour and the binocular needs of eye movements [24,30], synchronisation is very crucial and the fixational eye movements must be very coordinated. In Martinez-Cond's review [3] it was mentioned that *drift* has been reported to be both conjugate and non-conjugate.

The synchronisation properties of fixational eye movements raise many questions. In this study we address several of them. The first question to be addressed is what are the coupling relationships between the horizontal and vertical axis. These are controlled by different brain stem nuclei located on different sides of the brain. This directly relates to the properties of correlation and synchronisation between the right side and left side of the brain, in order to serve the three dimensional picture construction.

2 Persistence properties of horizontal and vertical fixational eye movements

2.1 Measurements and data

Data of five normal subjects was collected at the University of Potsdam. All procedures were in accordance with the Helsinki Declaration. All subjects gave written informed consent, had normal or corrected to normal vision, and are experienced participants in eye-tracking experiments. Eye movements for these participants were recorded using an EyeLink-II system with a sampling rate of $500\,\mathrm{Hz}$ and an instrument spatial resolution $< 0.01\,\mathrm{deg}$. The subjects were required to fixate a small stimulus with a spatial extent of $0.12\,\mathrm{deg}$ or $7.2\,\mathrm{arc\text{-}min}$ (3×3 pixels on a computer display, black square on a white background). This stimulus produced a rate of microsaccades similar to that obtained with a wide variety of other stimuli used in the same laboratory. Each participant performed 100 trials with a duration of 3 secs. During off-line processing some of the trials were discarded, for example if they contained saccades greater than one degree, leaving a total of 474 trials for further analysis [2]. All trials were identical, simple fixation, and thus the absence of a few trials for any one subject is inconsequential. The recording of each trial included position trajectories of horizontal and vertical components of left eye and right eye movements. Figure 1 shows a simultaneous recording of horizontal and vertical miniature eye movements for the left eye from one subject. The horizontal and vertical movements (upper and lower traces in the figure, respectively) exhibit an alternating sequence of slow drift and resetting microsaccades. Usually, the subjects show an individual preponderance regarding the direction of these drifts and resetting microsaccades. In this subject, for example, the drift in the horizontal movement occurred typically to the right and the microsaccades to the left (Fig. 1).

2.2 Method of analysis

To study some aspects of the dynamical behaviour of fixational eye movements, we employ the detrended fluctuation analysis (DFA) which was developed to quantify long-term power-law correlations embedded in a nonstationary time series [31,32]. The DFA method has been successfully applied to research fields such as cardiac dynamics [33–37], human gait [38], climate temperature fluctuations [39] and neural receptors in biological systems [40]. Here we apply this method to the velocity series derived from the position series of fixational eye movements.

For a position series x_i, $i = 1, \ldots, N + 1$, of a horizontal or vertical movement, we first calculate its velocity series v_i by $v_i = T_0(x_{i+1} - x_i)$, where T_0 is the sampling rate; in our
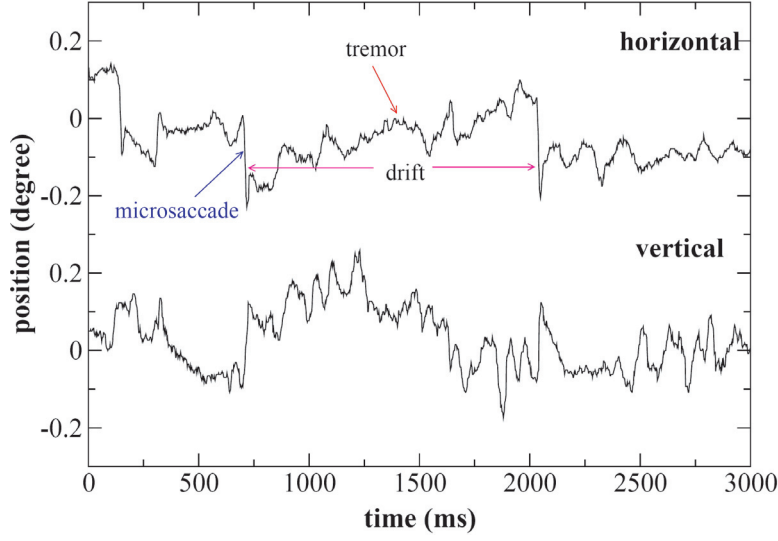
Fig. 1. (Colour online) simultaneous recording of horizontal and vertical position of left eye movements. The traces show microsaccades, drift and tremor in eye position. In the horizontal tracing, up represents right and down represents left; in the vertical tracing, up represents up and down represents down movements.

experiments $T_0 = 500$ Hz. We chose to use a two-point velocity in order to avoid any smoothing and clearly characterise the direction and magnitude of a movement. For other definitions of velocity see [17].

We first calculate the integrated series as a profile

$$Y(k) = \sum_{i=1}^{k} [v_i - \langle v \rangle], \qquad k = 1, \ldots, N. \tag{1}$$

Subtraction of the mean $\langle v \rangle$ of the whole series is not compulsory since it would be eliminated by the detrending in the third step [32]. Thus $Y(k)$ in Eq. (1) actually represents the "position".

We then divide the profile $Y(k)$ of N elements into $N_t = \text{int}(N/t)$ non-overlapping segments of equal length t, where $\text{int}(N/t)$ denotes the maximal integer not larger than N/t. Since the length N of the series is often not a multiple of the considered time scale t, a short part at the end of the profile may remain. In order not to disregard this part of the series, the same procedure is repeated starting from the opposite end. Therefore, $2N_t$ segments are obtained altogether.

Next, we determine in each segment the optimum polynomial fit of the profile and calculate the variance of the profile from these best polynomials

$$F^2(\nu, t) \equiv \frac{1}{t} \sum_{i=1}^{t} \{Y((\nu-1)t + i) - y_\nu(i)\}^2 \tag{2}$$

for each segment ν, $\nu = 1, \ldots, N_t$, and

$$F^2(\nu, t) \equiv \frac{1}{t} \sum_{i=1}^{t} \{Y(N - (\nu - N_t)t + i) - y_\nu(i)\}^2 \tag{3}$$

for $\nu = N_t + 1, \ldots, 2N_t$, where y_ν is the fitting polynomial in segment ν. If this fitting polynomial is linear, then it is the first-order detrended fluctuation analysis (DFA1). This eliminates the influence of possible linear trends in the profile on scales larger than the segment [31]. In general, in the nth order DFA (DFAn), y_ν is the best nth-order polynomial fit of the profile in segment
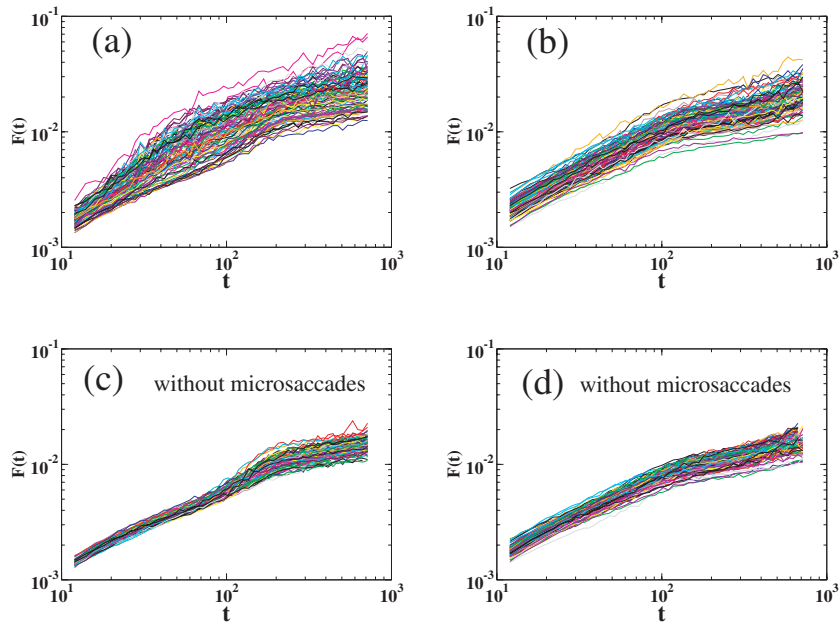
Fig. 2. (Colour online) detrended fluctuation analysis (DFA2) of velocity records of horizontal and vertical eye movements, from the right eye of a typical participant; the time units are milliseconds while F(t) units are in degrees: (a) horizontal; (b) vertical; (c) horizontal (same data as (a)) after removing microsaccades; (d) vertical (same data as (b)) after removing microsaccades.

ν. Therefore, linear, quadratic, cubic, or higher order polynomials can be used in the fitting procedure. Since the detrending of the original time series is done by the subtraction of the polynomial fits from the profile, different order DFA differ in their capability of eliminating trends of order $n - 1$ in the series.

Finally, the fluctuation $F(t)$ over the time windows of size t is determined as a root-mean-square of the variance

$$F(t) = \sqrt{\frac{1}{2N_t} \sum_{\nu=1}^{2N_t} F^2(\nu, t)}. \tag{4}$$

This computation is repeated over all possible interval lengths. Of course, in DFA $F(t)$ depends on the DFA order n. By construction, $F(t)$ is only defined for $t \geq n + 2$. For very large scales, e.g., for $t > N/4$, $F(t)$ becomes statistically unreliable because the number of segments N_t for the averaging procedure becomes very small. We therefore limit our results to $[n + 2, N/4]$.

Typically, $F(t)$ increases with interval length t. We determine the scaling behaviour of the fluctuations by analysing log-log plots of $F(t)$ versus t. A power law $F(t) \propto t^\alpha$, where α is a scaling exponent, represents the long-range power-law correlation properties of the signal. If $\alpha = 0.5$, the series is uncorrelated (white noise); if $\alpha < 0.5$, the series is anti-correlated; if $\alpha > 0.5$, the series is correlated or persistent.

2.3 Analysis and results of fixational eye movements

We applied DFA1 through DFA4 to all velocity records derived from the horizontal and vertical micro eye movements components. Since the scaling exponents of the fluctuation functions obtained by DFA1 through DFA4 are similar, we show here the DFA2 results as a representative of the DFA analysis.

As can be seen from Figs. 2(a) and (b) (see also Figs. 3(a) and (b)), the fluctuation functions of horizontal components have pronounced differences from the fluctuation functions of
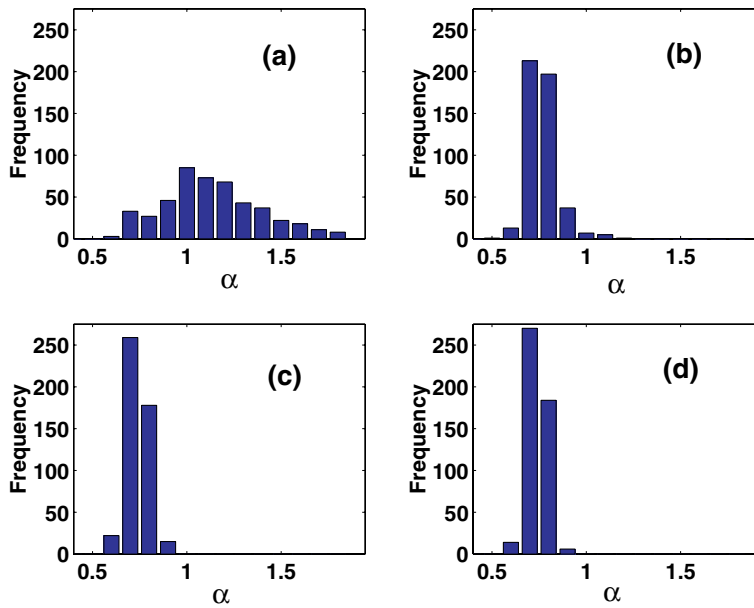
Fig. 3. Histograms of the number of trails having an exponent α, obtained by DFA2 at the short time scales (between $12\,\text{ms}$ and $40\,\text{ms}$) for all the horizontal and vertical trials (with duration of $3\,\text{sec}$) with and without microsaccades from the left eyes of all participants: (a) horizontal, (b) vertical, (c) horizontal without microsaccades and (d) vertical without microsaccades.

vertical components. This is expressed by several characteristics. There is a broader range of exponents in the horizontal compared to the vertical. The crossover times from large exponents (at short time scales) to smaller exponents (at large time scales) in horizontal, also show a broader range compared with the vertical ones. Moreover, the scaling exponents at short time scales (between $12\,\text{ms}$ and $40\,\text{ms}$) for horizontal are typically larger than the corresponding exponents for vertical as shown also in Figs. 3(a) and (b). However, if we remove microsaccades[2] the fluctuations of both components, the corresponding crossovers and the exponents at small time scales become similar (Figs. 2(c) and (d), 3(c) and (d)). This result indicates that microsaccades strongly influence the horizontal components in fixational eye movements. Note, the close similarity of the fluctuation function $F(t)$ in the different $3\,\text{sec}$ trials, in particular after removing the microsaccades, indicates that the scaling exponent is a stationary and significant characteristic of the eye movement. In Fig. 3 we show the histograms of the scaling exponents for the short time scales, for all trials with and without microsaccades from the left eyes of all participants. From this plot we notice that at the short time scale, the horizontal and vertical directions exhibit persistent behaviour ($\alpha > 0.5$), where the horizontal components show stronger persistence than the vertical. The average value of the scaling exponents for all trials is 0.76 for the vertical components and 1.1 for the horizontal components (see Table 1(a)). The scaling exponents of horizontal components show a broader distribution than the vertical components. However, after removing microsaccades the fluctuations of horizontal components and the corresponding scaling exponents have a pronounced change to a narrow distribution while the vertical components change very little (Figs. 2(b) and (d), 3(b) and (d)). When comparing the scaling exponents for the original horizontal series with the scaling exponents for the horizontal removed microsaccades series, we find that the scaling exponents decrease from an average value around 1.1 to 0.74, while for the vertical components the scaling exponents decrease from an average value around 0.76 to 0.74 (Table 1). Horizontal and vertical become similar after removing microsaccades. We find that at long time scales (between 300 and

---

[2] Microsaccades were detected from the velocity series. We removed velocities above a threshold of $15\,\text{deg/s}$. On average, between six and seven microsaccades are removed for each $3\,\text{sec}$ trial. The points were removed simultaneously from the vertical and horizontal data sets. For more details, see also [20].

Table 1. Average values of the scaling exponents obtained by DFA2 for all fixational eye movements we measured. HL = horizontal movements of left eyes, HR = horizontal movements of right eyes, VL = vertical movements of left eyes, and VR = vertical movements of right eyes.

component		Short time scale	Long time scale
(a)	HL	1.13 ± 0.26	0.29 ± 0.14
	HR	1.05 ± 0.25	0.31 ± 0.14
	VL	0.76 ± 0.08	0.34 ± 0.13
	VR	0.76 ± 0.09	0.30 ± 0.12
Microsaccades removed			
(b)	HL	0.74 ± 0.06	0.26 ± 0.11
	HR	0.73 ± 0.05	0.26 ± 0.10
	VL	0.74 ± 0.05	0.36 ± 0.14
	VR	0.74 ± 0.04	0.35 ± 0.13

600 ms), the horizontal and vertical components show anti-persistence behaviour, $\alpha < 0.5$ (see Table 1(a)), with no significant differences between them. After removing the microsaccades, the scaling exponents at the long time scales remain almost the same as before. The horizontal components become slightly less anti-persistent than the vertical (see Table 1(a)).

We thus conclude that microsaccades in the horizontal direction are more dominant than in the vertical direction in fixational eye movements. The microsaccades enhance the persistence mostly in the horizontal components at the short time scales. At the long time scales both horizontal and vertical components are anti-persistence and less affected by the microsaccades. To further test if the above results are indeed affected by microsaccades, we randomly removed parts of the series under study with the same length as the removed microsaccades and repeated the DFA analysis. We found that this procedure does not influence the scaling exponents. Thus, the scaling difference between the series with and without microsaccades is indeed due to microsaccades.

Finally, we tested if the effect of microsaccades can also be seen in the power spectral density. To this end we analysed the power spectra of the horizontal and vertical velocity series, for the right eye of a typical participant, for all trials with and without microsaccades. Results are shown in Figs. 4(a) and (b), where the microsaccades are included. The power spectral density of horizontal and vertical components are found to be different (Figs. 4(a) and (b)). After removing the microsaccades the components become similar (Figs. 4(c) and (d)). This finding also indicates that the effect of the microsaccades in the horizontal component is stronger than in the vertical. Note, that this effect is seen much clearer in the DFA curves where only a few trials (of 3 sec) are sufficient to distinguish between the horizontal and vertical eye movements.

3 Synchronisation decay of fixational eye movements

3.1 The synchronisation decay

A known effect in multi-component systems is the establishment of phase synchronisation between the components. Synchronisation analysis is relevant when the mechanisms which connect the components' dynamic are not clear. Revealing phenomena such as *phase synchronisation*, *phase locking* or *fixed time delay* between the signals can supply rich and useful information about the underlying dynamics. For example, the phase synchronisation method led to the identification of a group of neurons oscillating in close synchronisation with the observed tremor in Parkinson's disease [41], a discovery which led to a novel treatment for this condition. The phase synchronisation (PS), the weakest form of synchrony, thus implies the existence of a coupling and a relationship between phases of two *weakly interacting* systems, where the amplitudes may remain uncorrelated [42].

The phase synchronisation method uses the concept of analytic signals (AS) [30,43] which is useful for detecting the phase in periodic and semi-periodic signals [44]. By computing the
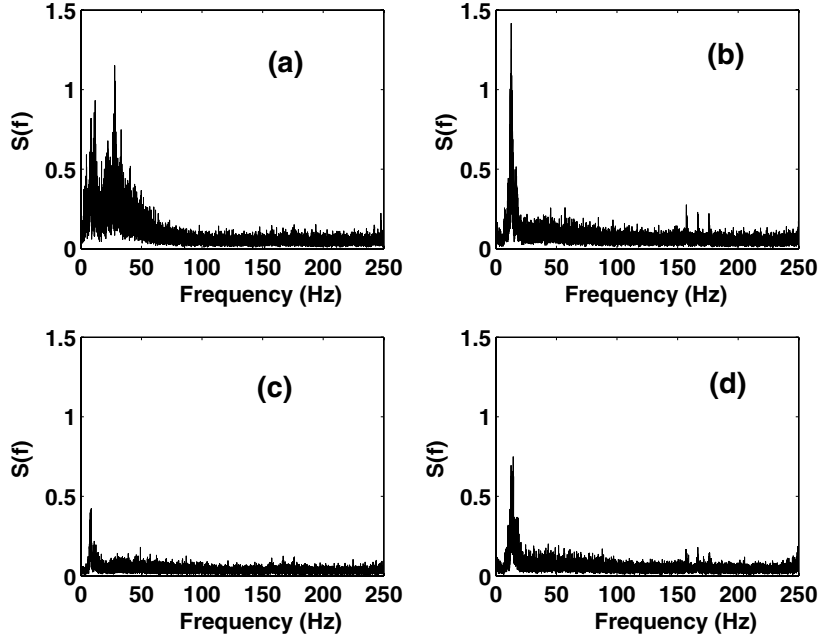
Fig. 4. Power spectral density $S(f)$ for the velocity series derived from the horizontal and vertical components from the right eye of one typical participant. (a) Horizontal with microsaccades; (b) vertical with microsaccades; (c) horizontal after removing the microsaccades; (d) vertical after removing the microsaccades.

AS $S_A = S(t) + iS_h(t)$ (where S is the original signal, and S_h is its Hilbert transform [45], see also Eq. (10)) of two simultaneous records S_a and S_b, and evaluating the phase differences series $\varphi_{n,m}(t) = n\phi_a(t) - m\phi_b(t)$ (where the phase $\phi_{a,b}$ is the angle of the AS in complex space, and $n : m$ are the integer relations between the natural frequencies of the signals). Phase synchronisation deals with the phase-lock condition that has to be fulfilled: $|\varphi_{n,m}(t) - \delta| <$ const., where δ is some average phase shift.

In noisy and chaotic systems, more typical of real world situations, we do not deal with pure phase locking, but rather with phase locking in a statistical manner. However, the generalised definition of phase locking, which can be applied to the case of chaotic and noisy oscillators, is based on the requirement that the time variations in the instantaneous phase difference are bounded [42, 44, 46]. We understand synchronisation of noisy systems as appearances of peaks in the distribution of the cyclic relative phase $\Psi_{n,m} = \varphi_{n,m} \bmod 2\pi$, that enables us to detect preferred values of the phase difference irrespective of the noise-induced phase jumps.

There are numerous possible methods for measuring how flat the distribution $P(\Psi_{n,m})$ is (see [41]). Tass et al. [47] were the first to introduce the concept of *Shanon Entropy* for evaluating synchronisation in noisy and chaotic systems. They found it useful to quantify the deviation of the actual distribution of the relative phase from a uniform one.

The benefit of using entropy is that it is a conventional estimate of the number of phase cells the system visits. For statistical mechanics to be applicable we need to work with coarse grained cells, for calculating the distribution $P(\Psi_{n,m}(t))$. Doing so, our entire range is $[0, 2\pi]$, and we have N cells each of the size of $\Delta = 2\pi/N$. The number of samples in cell k is

$$p_k = \frac{1}{n} \sum_i [\Theta(\Psi_{n,m}(t_i) - k\Delta) - \Theta(\Psi_{n,m}(t_i) - (k-1)\Delta)], \qquad k = 0, \dots, N-1, \qquad (5)$$

where t_i is the time at which sample i was taken, p_k is actually the relative frequency (or the probability) that the signals' phase difference stay in cell k, and n is the record length. $\Theta(x)$

is the Heaviside function, $\Theta(x) = 0$ for $x \leq 0$ and $\Theta(x) = 1$ for $x > 0$. The *Shanon entropy* is defined as:

$$S = -\sum_{k=1}^{N} p_k \log p_k \tag{6}$$

Equations (5) and (6), serve not only for defining a *synchronisation index*, but also as the algorithm we use to find synchronisation between two phases series (which we get from analytic signals). The only undefined parameter here is the number of cells (or bins). The optimal cells number N is given by

$$N = \exp[0.626 + 0.4 \log(n - 1)] \tag{7}$$

(see [48] or footnote on p. 20 in [41]). Therefore, the distribution of the differences series is then evaluated and the degree of phase synchronisation is calculated according to its Shannon entropy.

The *synchronisation index* is defined as,

$$\rho_{n,m} = \frac{S_{max} - S}{S_{max}}, \tag{8}$$

where $S_{max} = \log N$ is the maximum Shanon entropy.

In conclusion, a highly biased system (high entropy) would correspond to an independence between the components, and a narrow distribution (small entropy) would correspond to a strong phase synchronisation between them. The synchronisation index fulfills: $0 \leq \rho_{n,m} \leq 1$, where $\rho_{n,m} = 0$ corresponds to a uniform distribution (no synchronisation) and $\rho_{n,m} = 1$ corresponds to a distribution localised in one point (δ-Dirac-like distribution). Such distributions can be observed only in the ideal case of phase locking of noise-free quasi-linear oscillators.

In our case we would like to rescale the *synchronisation index* in order to take into account the artifact of asymmetry and nonstationarity. We would like to see how our signals correspond to each other in comparison to signals with the same deficiencies which are known to be un-coupled [24,30]. Moreover, the concept of synchronisation index could not be a standalone synchronisation test because there could exist in nature two systems that are "artificially" synchronised without any coupling between them. As a simple example, for any two sine functions (whose frequencies ratio is a rational number), a phase lock relation can be found in between. However, these two functions need not to be coupled and do not exhibit "real" synchronisation. An example of a noisy system, is that for any heartbeat rhythm and any clock one will be able to find a synchronisation relationship.

Therefore, we use the concept of the "synchronisation decay" [24,30,49]. This concept assumes that because the coupling is local in time, finding the synchronisation of the first time series with the future (and past) of the second time series will give a synchronisation value that is related to the geometric structure of the signal, and not to the influence of the signals on each other. The decay of synchronisation is therefore just a plot of the "simple synchronisation indices" as a function of the time delay. The algorithm we use to estimate the decay of synchronisation is:

1. Take the signals $s_1(t)$, $s_2(t - \tau)$ where

$$t \in \begin{cases} [0, N - \tau_{max} - 1] & \text{if } \tau < 0 \\ [\tau_{max}, N - 1] & \text{if } \tau \geqslant 0 \end{cases} \tag{9}$$

and $\tau \in [-\tau_{max}, \tau_{max}]$.

2. Evaluate the analytic signals (AS)

$$S_A^\tau(t) = S^\tau(t) + iS_H^\tau(t) = S^\tau(t) + \frac{i}{\pi q} * S^\tau(q) \tag{10}$$

where $S_H^\tau(t)$ is the Hilbert transform [45] of $S^\tau(t)$, the superscript τ represents the time shift that is taken between the signals, and "$*$" is a convolution with the integration

variable q. Evaluation is done using the AS form in the frequency domain

$$\int dt \, e^{-2\pi i f t} \left(S(t) + i \int dq \frac{S(q)}{\pi(t-q)} \right) = \iint dt \, dq \, e^{-2\pi i f t} S(q) \left(\delta(t-q) + \frac{i}{\pi(t-q)} \right)$$

$$= \left(\delta(q) + \frac{i}{\pi q} \right) * S(q) = (1 + \operatorname{sgn}(f))\mathbf{S}(f) = 2\Theta(f)\mathbf{S}(f) \tag{11}$$

where $\Theta(x)$ is the Heaviside function and $\mathbf{S}(f)$ the Fourier transform of S.

3. The analytic signals can be represented in the form $S_A^\tau(t) = A(t)\exp(i\phi^\tau(t))$. The phase series $\phi^\tau(t)$ can be easily obtained by the trigonometric relation

$$\phi^\tau(t) = \arctan\left(\frac{S_H^\tau(t)}{S^\tau(t)} \right) + \frac{\pi}{2}(1 - sgn(S^\tau)). \tag{12}$$

4. Calculate the series

$$\psi_{m,n}^\tau(t) = mod_{2\pi}\left(m\phi_1^\tau(t) - n\phi_2^\tau(t) \right) \tag{13}$$

where m, n are integers ($\neq 0$). The ratio m:n equals to the ratio between the dominant frequencies $\omega_2 : \omega_1$. One should choose m and n based on the physical properties (e.g., if both oscillators are theoretically similar, one should choose $\omega_2 : \omega_1 = 1$ and hence $m = n = 1$) and on the dominant peaks in the power spectrum of the records.

5. Evaluate the probability density P of $\psi_{m,n}^\tau(t)$, by choosing a fine division of $[0, 2\pi]$ to N_b bins (as described in [48]), and evaluating the probability P_k of finding $\psi_{m,n}^\tau(t)$ within the k-th bin.[3]

6. Evaluate the Shannon entropy [50] of the probability histogram

$$S^\tau = -\sum_i P_k \log P_k \tag{14}$$

Derive the synchronisation index ρ [47] by scaling the entropy S^τ to be in $[0,1]$, where 0 stands for lack of synchronisation and 1 stands for full synchronisation, using the relation

$$\rho^\tau = \frac{S_{max} - S^\tau}{S_{max}} \tag{15}$$

with $S_{max} = \log N_b$.

7. Set $\tau = \tau + 1$, return to step 1.

The algorithm should be applied on relatively short time scales so that the slips of the centre of the AS ring can be ignored. In order to avoid using the edges of each window (because estimation of the Hilbert transform is poor at the edge), the window should contain a few cycles more than the maximal window size allowed due to the slipping of the centre criterion (allowing us to crop the edges after the transform is done). The decay of the synchronisation index for all time windows should be averaged over all windows. A detailed picture of the development of coupling in time can be achieved by observing the individual time windows.

A "synchronised state" is a local state. It occurs when the synchronisation index ρ^τ vs. time shift τ has two significantly falling tails and one or a few maxima (e.g., see Fig. 5). A well pronounced synchronisation occurs when the difference between the tails and the maxima is larger than the standard deviation of the tails. We quantify the significance by evaluation of:

$$\frac{\langle \rho_{i\in\,\mathtt{middle}} \rangle - \langle \rho_{i\in\,\mathtt{tails}} \rangle}{\sqrt{\langle \rho_{i\in\,\mathtt{tails}}^2 \rangle - \langle \rho_{i\in\,\mathtt{tails}} \rangle^2}}. \tag{16}$$

---

[3] In a noise free periodic system when the two oscillators are phase-locked, $\psi_{m,n}$ satisfies the relation $|\psi_{m,n}^0(t) - \delta| < \epsilon$ for a certain δ where $\epsilon < 2\pi$ for all t, thus $P_k = 0$ for all bins outside the δ-zone.
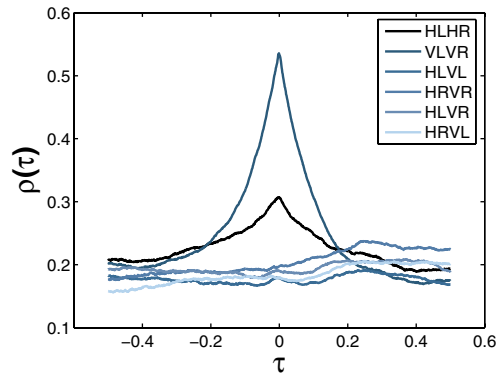
Fig. 5. (Colour online) synchronisation index ρ versus time delay τ (units of seconds) of fixational eye movements of the six combinations. It can be noticed that the horizontal left versus horizontal right [HLHR] (black line) and vertical left versus the vertical right [VLVR] show decay plot which are pointing a time synchronisation. However, the other four possibilities remain almost flat, indicating that they are not synchronised. The lines are: horizontal lest versus vertical left [HLVL]; the horizontal right versus vertical right [HRVR]; horizontal left versus vertical right [HLVR]; horizontal right versus vertical left [HRVL].

We consider the regions of τ where the synchronisation index ρ^τ stabilises as "tails", and the other regions of τ in the centre. We define the thresholds of the centre region for our records (see Fig. 5) so that the centre is exactly half of the time window. If one sets $\tau_{max} = 0$ and takes only one window, then the method reduces to the standard phase synchronisation method (and the significance will be infinite).

3.2 Measurements and data

Data from 10 normal subjects was produced by two measurement methods. Five subjects were measured by the EyeLinkII system, the same subjects as described above in section 2.1. The others were measured by the Scleral Magnetic Search Coil system, as follows. Data was collected from five (different) normal subjects (ages between 25–45 years old) who were students at Bar Ilan University or Beilinson Medical Center staff. All procedures were in accordance with the Helsinki Declaration. All subjects gave written informed consent, had normal or corrected to normal vision, and were naive to the purpose of the experiment. Horizontal and vertical movements of both eyes were recorded at a sampling rate of 1000 Hz and an instrument spatial resolution < 0.01 deg. The subjects were required to fixate a small laser spot rear projected onto a semitranslucent screen located 1 m in front of them, while their head was immobilised by soft pads firmly attached to the chair.

Each participant performed 4 to 6 trails of 1 min duration.

3.3 Analysis and results

The results provide important information regarding fixational eye movements. By examining the "synchronisation decay" diagrams it can be observed that although the synchronisation indexes were high, only several axes were coupled.

Plotting the raw data of the fixational eye movements (as horizontal vs. vertical) position (see Fig. 6), reveals that the trajectories in the two eyes are slightly different. We can deduce that the images projected on the retina travelled over slightly different regions on the left and right eyes.

In order to test the synchronisation of the binocular fixational movements, we applied the phase synchronisation decay method (see section 3.1), to all six possibilities of the fixational
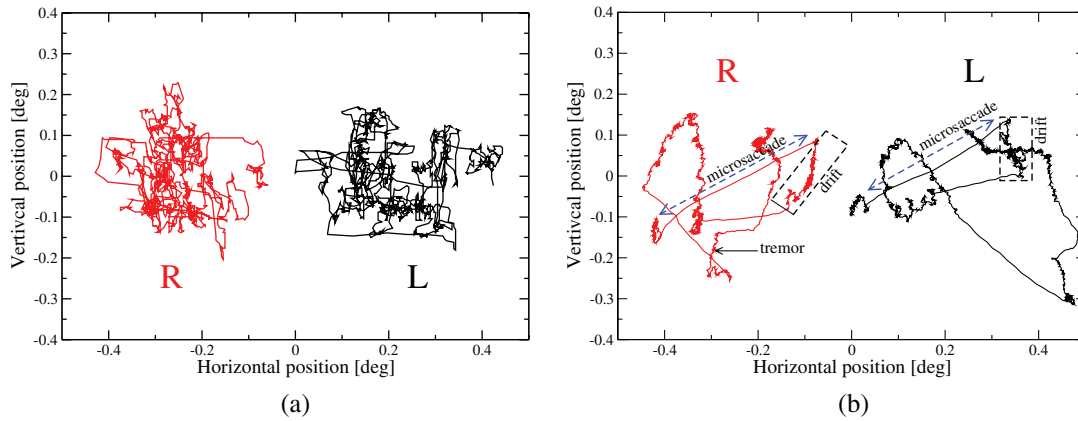
Fig. 6. (Colour online) simultaneous recording of vertical and horizontal position of left and right eye movements (vertical versus horizontal). (a) Recorded by video EyeLinkII system (the same trail as in Fig. 1). (b) Recorded by magnetic scleral coil system, microsaccades-signed by arrows drift-signed by dashed box and tremor. The tracks show micro eye movements (microsaccades drift and tremor) in two dimensions. It can be noticed in (a) and (b), that the tracks (right eye signed by red coloured R-capital letter, and left eye signed by black coloured L-capital letter) are different and not completely similar. The eyes "travelled" simultaneously but not completely respectively on the "same" sites on the retina.
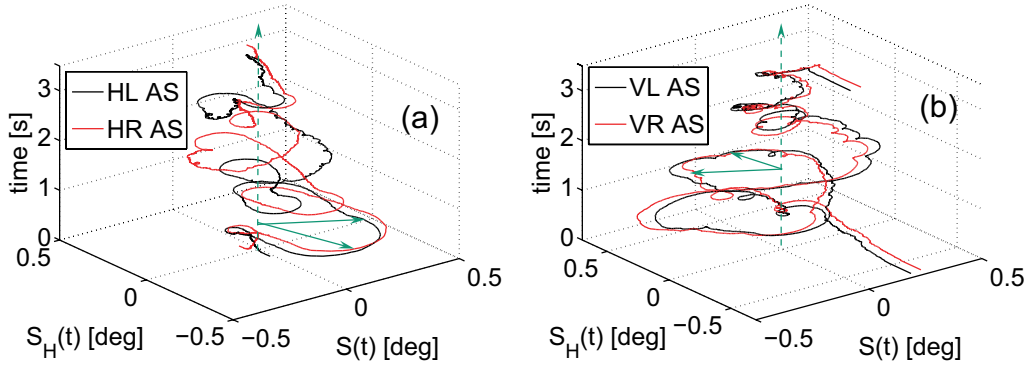

Fig. 7. (Colour online) examples of record's analytic signal function of time, of the horizontal position components (a) and vertical position components (b); in figure (a) the horizontal components (the left and right horizontal eye movements) analytic signals are not correspondingly oscillates, however, the vertical components are well oscillating in harmony.

eye movements axes (except torsional). The possible combinations are the following: (1) the right eye horizontal and left eye horizontal; (2) right eye vertical and left eye vertical; (3) right eye horizontal and left eye vertical; (4) right eye vertical and left eye horizontal; (5) left eye horizontal and left eye vertical; (6) right eye horizontal and left eye vertical.

To calculate the average synchronisation decay for every record of eye movement for the measured magnetic coil records and for the video measurements, we divided each given fixational eye movement record into windows with duration time of 3 sec (see method section 3.1). The records measured by video are divided into trials of the same duration (3 sec, see section 2.1). In Fig. 7 we present an example of an analytic signal $(s(t), s_{hilbert}(t))$ versus time for one window from a record. Figure 7(a) shows the analytic signal of the horizontal axes (horizontal left and horizontal right) and in Fig. 7(b) are the vertical axes. We can remark that the horizontal analytic signal's axes (shown in Fig. 7(a)) are cycled differently from each other while the vertical (in Fig. 7(b)), cycled almost together.

Calculating the average $\rho(\tau)$ of all windows for the time records (of video and magnetic coil records), through testing all 6 combinations, we find that only two combinations are synchronised. Figure 5 exhibits representative results for all six combinations. It can be seen that except for the horizontal-horizontal (black line), and vertical-vertical (top blue line) which are
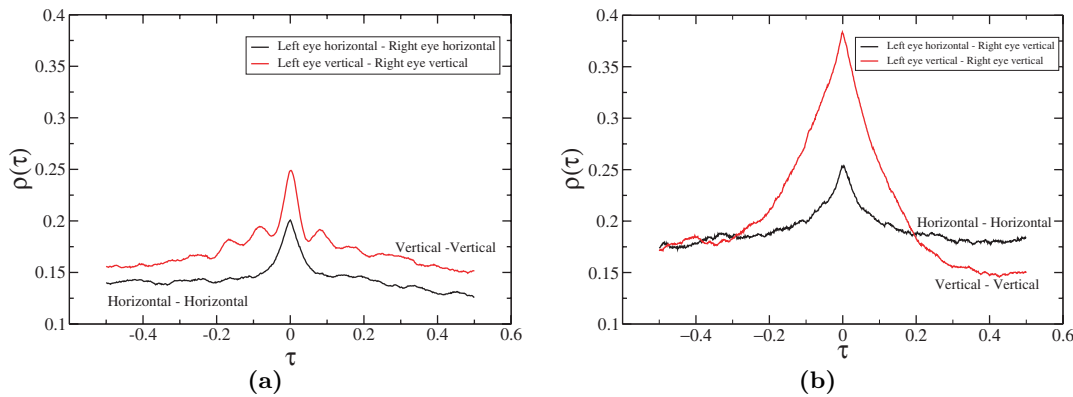
Fig. 8. (Colour online) synchronisation index ρ versus time delay τ (units of seconds). (a) Synchronisation decay between left and right eyes horizontal (black line) and vertical (red line) of video camera measurements results. (b) Synchronisation decay between left and right eyes horizontal (black line) and vertical (red line) of scleral magnetic coil measurement results. There are clearly decaying tails for both (the horizontal and vertical in both measurements methods). It can been seen that the vertical components are more synchronised than the horizontal since their decay time is shorter and their amplitudes (the height of the maximum peak from the background) are higher.

synchronised, all the other combinations are not. Their decay plots demonstrate decay in time (for $\pm\tau$), however, the others are almost flat or fluctuate around a flat line, although the index $\rho(\tau)$ maintains a high value. In summary, the results show that the horizontal left and right and the vertical left and right are the only synchronised combinations. However, the vertical left and vertical right are more synchronised than the horizontals.

Figures 8(a) and (b) show the synchronisation index $\rho(\tau)$ (versus the time delay τ in units of milliseconds). This figure exhibits the synchronisation decay plot of two representative subjects (shown in Figs. 6(a) and (b)) that had been measured using the two methods. Only two movement axes were synchronised, the vertical left versus vertical right (represented by a red line in Figs. 8(a) and (b) and horizontal left and horizontal right (black line). Both are synchronised (vertical-vertical and horizontal-horizontal), however for the vertical-vertical the decay is more pronounced since its decay amplitude and velocity are larger, meaning that it is significantly synchronised.

In Fig. 9 we summarise the synchronisation decay significance for all 10 subjects. We plot in Fig. 9(a) the video measurement results and in Fig. 9(b) the magnetic coil measurements results. Each box in the figures is related to one subject (where each subjects' records were divided into half and are represented by two bars).

A value higher than 2 (above the dashed line in the plots), indicates a pronounced synchronisation. It can be noticed that all subjects' eye movement records are synchronised in the vertical-vertical (marked by red circles) and horizontal-horizontal (marked by boxes). Furthermore, there is a significant difference in the synchronisation of the vertical axes compared to the horizontal, where the vertical axes are significantly higher: we can see that the boxes are significantly above the circles. However, it shows that these two combinations were synchronised in all subjects and that four of the five always showed greater synchronisation in the vertical that the horizontal.

4 Discussion

When the visual world is stabilised on the retina, visual perception fades as a consequence of neural adaptation. During normal vision we continuously move our eyes involuntarily even as we try to fixate our gaze on a small stimulus, preventing retinal stabilisation and the associated fading of vision [3]. The nature of the neural activity correlated with microsaccades at different levels in the visual system has been a long standing controversy in eye-movement
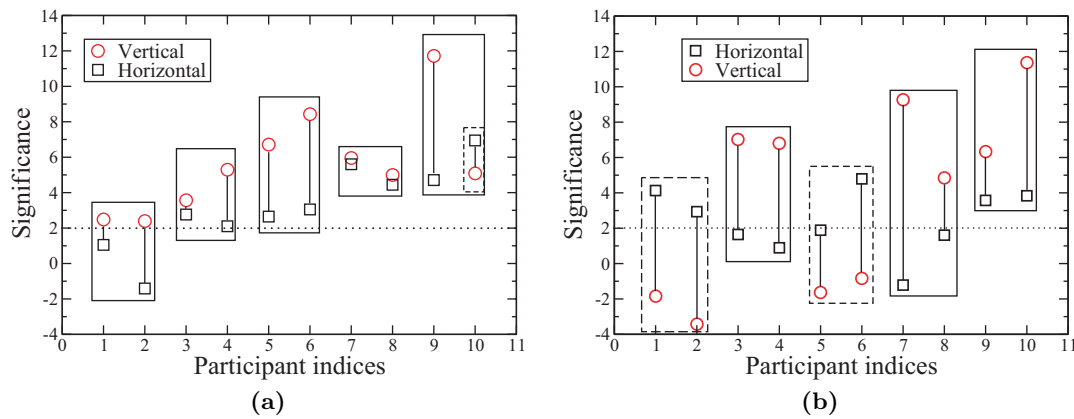
Fig. 9. (Colour online) synchronisation decay significance (considered synchronised if greater than 2) of ten normal subjects. Each participant' records were divided in half and are represented by two bars. The *red circles* presents significance between vertical-vertical, and the *black squares* present significance between horizontal-horizontal. (a) Synchronisation significance of video Eye-LinkII measurements. (b) Synchronisation significance of scleral magnetic coil measurements. Note that the significance for vertical components are higher than horizontal, indicating that the vertical component are more synchronised. However, two from five participants whose their micro-eye movements were measured by magnetic coil method showed the opposite.

research. Steinman et al. [51] showed that a person may select not to make microsaccades, and still be able to see the object of interest, whereas Gerrits & Vendrik [52] and Clowes [53] found that optimal viewing conditions were only obtained when both microsaccades and drifts were present. Since microsaccades can be suppressed voluntarily in high acuity observation tasks [25,54], it was concluded that microsaccades serve no useful purpose and even that they represent an evolutionary puzzle [17].

4.1 Scaling of horizontal and vertical fixational eye movements

Our study using DFA suggests that microsaccades play different roles on different time scales in vertical and horizontal components in the corrections of the fixational eye movements, consistent with [2]. Moreover we show that due to microsaccades there is also different scaling behaviour between the horizontal and the vertical fixational eye movements. Our results suggest that microsaccades at short time scales enhance the persistence mostly in horizontal movements and much less in the vertical movements.

Our finding that the persistence in horizontal and vertical fixational eye movements, which are controlled by different brain stem nuclei, exhibit pronounced different behaviour also suggests that the role of microsaccades in horizontal movements are more dominant. These findings may provide better understanding of the recent neurophysiological findings on the effects of microsaccades on visual information processing [55].

4.2 Fixational eye movements synchronisation

We presented a new technique to study the synchronisation between various components of eye movements. This technique is more sensitive for detecting weak phase synchronisation in nonstationary data sets. We analysed the synchronisation in fixational eye movements for all six possibilities of synchronisation between eyes components. For all subjects it was found that the vertical axes and horizontal axes are the only two combinations that are synchronised. Furthermore, we found that there is a significant difference in synchronisation between the horizontal and vertical components, the vertical components in both eyes are more synchronised than the horizontal ones.
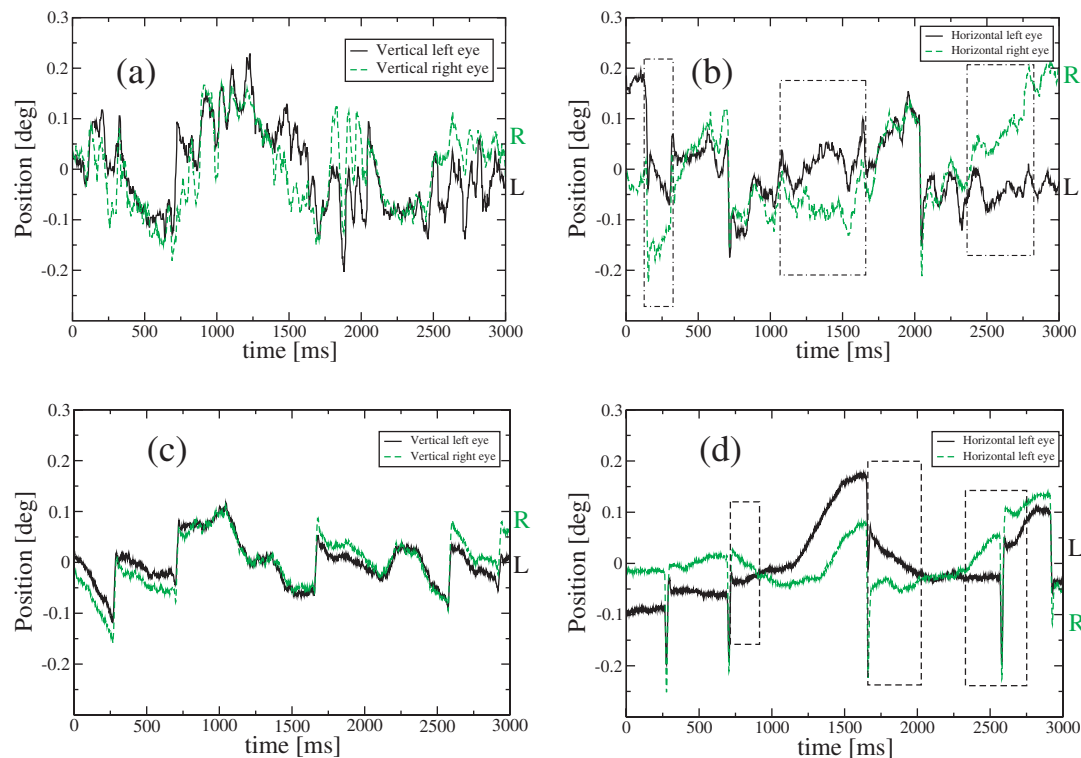
Fig. 10. (Colour online) a typical 3 sec record of eye position as a function of time in the (a) vertical and (b) horizontal planes (measured by EyeLinkII). (c) Vertical and (d) horizontal planes (measured by Scleral Magnetic coil). Note that the vertical components are always conjugate (i.e., are coupled), whereas in the horizontal plane, there are regions of dis-conjugacy, that is, in anti-phase (see enclosed areas).

These results suggest that the vertical movements are stronger coupled when compared to the horizontal movements (see Fig. 10). This difference may be based on the need for disconjugate eye movements in the horizontal plane in order to match the stereoscopic image for different viewing distances, a need not found in the vertical plane. However, we found three subjects (out of total 10 measured by video and magnetic coil methods) who had horizontal components that were more synchronised than the vertical (see dashed boxes in Figs. 9(a) and (b)), implying that this relationship is not trivial and there is need for further studies.

References

1. L.A. Riggs, F. Ratliff, J.C. Cornsweet, J. Opt. Soc. Am. **43**, 495 (1953)
2. R. Engbert, R. Kliegl, Psychol. Sci. **15**, 431 (2004)
3. S. Martinez-Conde, S.L. Macknik, D.H. Hubel, Nature Rev. Neurosci. **5**, 229 (2004)
4. D. Coppola, D. Purves, PNAS **93**, 8001 (1996)
5. B.P. Ölveczky, S.A. Baccus, M. Meister, Nature **423**, 401 (2003)
6. R. Engbert, Progr. Brain Res. **154**, 177 (2006)
7. E. Ahissar, A. Arieli, Neuron **32**, 185 (2001)
8. A. Spauschus, J. Marsden, D.M. Halliday, J.R. Rosenberg, P. Brown, Exp. Brain Res. **126**, 556 (1999)
9. L.A. Riggs, F. Ratliff, Science **114**, 17 (1951)
10. R.W. Ditchburn, B.L. Ginsborg, J. Physiol. (Lond.) **119**, 1 (1953)
11. T.N. Cornsweet, J. Opt. Soc. Am. **46**, 987 (1956)
12. J. Nachmias, J. Opt. Soc. Am. **49**, 901 (1959)

13. J. Nachmias, J. Opt. Soc. Am. **51**, 761 (1961)
14. R.M. Steinman, R.J. Cunitz, G.T. Timberlake, M. Herman, Science **155**, 1577 (1967)
15. G.J.St. Cyr, D.H. Fender, Vision Res. **9**, 245 (1969)
16. A.R. Shakhnovich, J.G. Thomas, Electroencephalogr. Clin. Neurophysiol. **42**, 117 (1977)
17. R. Engbert, R. Kliegl, Vision Res. **43**, 1035 (2003)
18. R.H.S. Carpenter, *Movements of the Eyes*, 2nd edn. (Pion Ltd., London, 1988)
19. R. Engbert, K. Mergenthaler, PNAS **103**, 7192 (2006)
20. J.R. Liang, S. Moshel, A.Z. Zivotofsky, A. Caspi, R. Engbert, R. Kliegl, S. Havlin, Phys. Rev. E **71**, 031909 (2005)
21. R. Engbert, R. Kliegl, *The Mind's Eyes: Cognitive and Applied Aspects of Eye Movements* (Elsevier, Oxford, 2003), p. 103
22. K. Mergenthaler, R. Engbert, Phys. Rev. Lett. **98**, 138104 (2007)
23. M. Rolfs, R. Engbert, R. Kliegl, Psychol. Sci. **15**, 705 (2004)
24. S. Moshel, J. Liang, A. Caspi, R. Engbert, R. Kliegl, S. Havlin, A.Z. Zivotofsky, Ann. NY Acad. Sci. **1039**, 484 (2005)
25. R. Bridgeman, J. Palca, Vis. Res. **20**, 813 (1980)
26. D.L. Sparks, Nature Rev. Neurosci. **3**, 952 (2002)
27. M. King, W. Zhou, Anat. Rec. (New Anat.) **261**, 153 (2000)
28. W. Zhou, W.M. King, Nature **393**, 692 (1998)
29. L.A. Riggs, F. Ratliff, Science **40**, 687 (1950)
30. G. Gozolchiani, S. Moshel, J.M. Hausdorff, E. Simon, J. Kurths, S. Havlin, Physica A **366**, 552 (2006)
31. C.-K. Peng, S.V. Buldyrev, S. Havlin, M. Simons, H.E. Stanley, A.L. Goldberger, Phys. Rev. E **49**, 1685 (1994)
32. J.W. Kantelhardt, E. Koscielny-Bunde, H.H.A. Rego, S. Havlin, A. Bunde, Physica A **295**, 441 (2001)
33. C.-K. Peng, S. Havlin, H.E. Stanley, A.L. Goldberger, Chaos **5**, 82 (1995)
34. A. Bunde, S. Havlin, J.W. Kantelhardt, T. Penzel, J.H. Peter, K. Voigt, Phys. Rev. Lett. **85**, 3736 (2000)
35. P.Ch. Ivanov, M.G. Rosenblum, C.-K. Peng, J.E. Mietus, S. Havlin, H.E. Stanley, A.L. Goldberger, Nature **383**, 323 (1996)
36. P.Ch. Ivanov, A. Bunde, L.A.N. Amaral, S. Havlin, J. Fritsch-Yelle, R.M. Baevsky, H.E. Stanley, A.L. Goldberger, Europhys. Lett. **48**, 594 (1999)
37. Y. Ashkenazy, P.Ch. Ivanov, S. Havlin, C.-K. Peng, A.L. Goldberger, H.E. Stanley, Phys. Rev. Lett. **86**, 1900 (2001)
38. J.M. Hausdorff, C.-K. Peng, Z. Ladin, J.Y. Wei, A.L. Goldberger, J. Appl. Physiol. **78**, 349 (1995)
39. R.A. Monetti, S. Havlin, A. Bunde, Physica A **320**, 581 (2003)
40. S. Bahar, J.W. Kantelhardt, A. Neiman, H.H.A. Rego, D.F. Russell, L. Wilkens, A. Bunde, F. Moss, Europhys. Lett. **56**, 454 (2001)
41. M.G. Rosenblum, A.S. Pikovsky, C. Schäfer, P.A. Tass, J. Kurths, *Neuro-informatics and Neural Modelling. Handbook of Biological Physics*, edited by F. Moss, S. Gielen, A.J. Hoff, Vol. 4 (Elsevier, North-Holland, 2001), p. 279
42. M.G. Rosenblum, A.S. Pikovsky, J. Kurths, Phys. Rev. Lett. **76**, 1804 (1996)
43. D. Gabor, J. IEEE (London) **93**, 429 (1946)
44. A. Pikovsky, J. Kurths, M. Rosenblum, *Synchronization: A Universal Concept in Nonlinear Sciences* (Cambridge University Press, Cambridge, 2001)
45. R. Bracewell, *The Fourier Transform and Its Applications*, 2nd edn. (McGraw-Hill, 1986)
46. V.S. Anishchenko, V.V. Astakhov, A.B. Neiman, T.E. Vadivasova, L. Schimansky-Geier, *Nonlinear Dynamics of Chaotic and Stochastic Systems* (Springer-Verlag, Berlin, 2003)
47. P. Tass, M.G. Rosenblum, J. Weule, J. Kurths, A. Pikovsky, J. Volkmann, A. Schnitzler, H.-J. Freund, Phys. Rev. Lett. **81**, 3291 (1998)
48. R.K. Otnes, L. Enochson, *Digital Time Series Analysis* (Wiley-Interscience, New York, 1972)
49. D. Rybski, S. Havlin, A. Bunde, Physica A **320**, 601 (2003)
50. C.E. Shannon, Bell Sys. Tech. J. **27**, 379 (1948); Bell Sys. Tech. J. **27**, 623 (1948)
51. R.M. Steinman, G.M. Haddad, A.A. Skavenski, D. Wyman, Science **181**, 810 (1973)
52. H.J.M. Gerrits, A.J.H. Vendrik, Vision Res. **10**, 1443 (1970)
53. M.B. Clowes, Opt. Acta. **9**, 65 (1962)
54. B.J. Winterson, H. Collewijn, Vision Res. **16**, 1387 (1976)
55. S. Martinez-Conde, S.L. Macknik, D.H. Hubel, Nature Neurosci. **3**, 251 (2000)